A 24-GHz Portable FMCW Radar with Continuous Beam Steering Phased Array for Short-Range Localization

Zhengyu Peng, *Student Member, IEEE*, Lixin Ran, and Changzhi Li, *Senior Member, IEEE*

***Abstract*—This paper presents a 24-GHz portable frequency-modulated continuous-wave (FMCW) radar transceiver with continuous beam steering phased array for short-range localization. The transmitter channel of the proposed radar consists of a free-running voltage controlled oscillator (VCO) and a single patch antenna. A cost-effective analog "sawtooth" voltage generator is used to control the VCO to produce frequency-modulated radar signal while maintaining coherent detection. The receiver channel has a phased array, a six-port circuit and a baseband circuit. The phased array is a 4-element linear array. Each element is a series-fed microstrip patch array antenna. The beam of the phased array can be continuously steered with a range of ±30° on the H-plane through an array of vector controllers. The vector controller is based on the concept of vector sum with binary-phase-shift attenuators. Each vector controller is capable of controlling the phase and the amplitude of the corresponding array element of the 4-element linear array. The beat signal of the FMCW radar is detected by the six-port circuit and then sampled by a soundcard of a laptop. The entire radar system is fabricated on printed circuit boards (PCB). The design principles of the binary-phase-shift attenuator, the vector controller, and the radar system are discussed. Calibration method of the array is introduced to minimize the errors caused by component variation and fabrication. The radiation patterns of the phased array have been measured. Experiment results show that the proposed solution is suitable for short-range localization.**

***Index Terms*—FMCW radar, phased array, continuous beam steering, vector controller, localization.**

I. Introduction

APPLICATIONS of radar system have been extended to commercial areas, such as driver assistance [1], [2], industrial localizations [3], through-wall detections [4], [5] and biomedical applications [6]–[8]. Typically, mechanical steering system or phased array is necessary for a radar system to perform a two-dimensional or three-dimensional scan. It is known that the mechanical steering system will increase the size, weight and cost while limiting the reliability of the whole system. For consumer electronics, the size of the system is usually essential in order to be mounted on existing devices and equipment, such as automobiles and medical instrument, without affecting their profiles and functions. Phased array radar systems, which feature lighter weight, lower profile and higher steering speed [9], overcome the drawbacks of mechanical beam steering systems. However, a conventional phased array is expensive, especially at frequencies above the K-band. This is mainly because conventional solutions require high-frequency phase shifters, which are expensive and have a small number of manufacturers. New beamforming techniques are emerging for higher frequencies. One of the simplest approaches to realize beam steering at frequencies higher than 24 GHz is using delay methods and radio frequency (RF) switches [10]–[12]. However, these methods usually have limited number of steering angles, and the signal routing will be troublesome with the increase of steering angles. Other techniques, such as local oscillator (LO) phase-shifting [13], [14] and vector modulator [15], [16], are based on solid state circuits. The LO phase-shifting technique requires a complex multi-phase VCO and multiple phase select switches. Its steering angles are also discrete. The vector modulator technique based on the concept of vector sum [17]–[19], which features continuous phase and amplitude control capabilities, is a good alternative for high frequency phase shifters.

Regarding radar systems, continuous-wave (CW) radars have advantages of low transmit power, simple structure, and high sensitivity, which enable broad applications in various areas. The frequency-modulated continuous-wave (FMCW) radar is one of the most popular CW radar types [20]–[23] with the capability to obtain absolute range information of targets. Transceiver architecture based on six-port [24] features simple structure and high performance, and has been used in biomedical interferometry radars [25], [26] and FMCW radars [27], [28].

In this paper, a 24-GHz portable FMCW radar with continuous beam steering phased array is proposed. The proposed radar system includes both the transmitter and receiver channels. The transmitter channel consists of a VCO and a single patch antenna. A "sawtooth" voltage generated by an operational-amplifier based circuit is used to control the VCO to generate a frequency-modulated RF signal from 24.35 GHz to 24.75 GHz. The receiver channel consists of a phased

Manuscript submitted on May 10, 2016. This work was supported by the NSF under grant ECCS-1254838 and the NSFC under grant 61528104.

Z. Peng and C. Li are with the Department of Electrical and Computer Engineering, Texas Tech University, Lubbock, TX 79409 USA (e-mail: zhengyu.peng@ttu.edu; changzhi.li@ttu.edu).

L. Ran is with the Laboratory of Applied Research on Electromagnetics (ARE), Zhejiang University, Hangzhou 310027, China (e-mail: ranlx@zju.edu.cn).

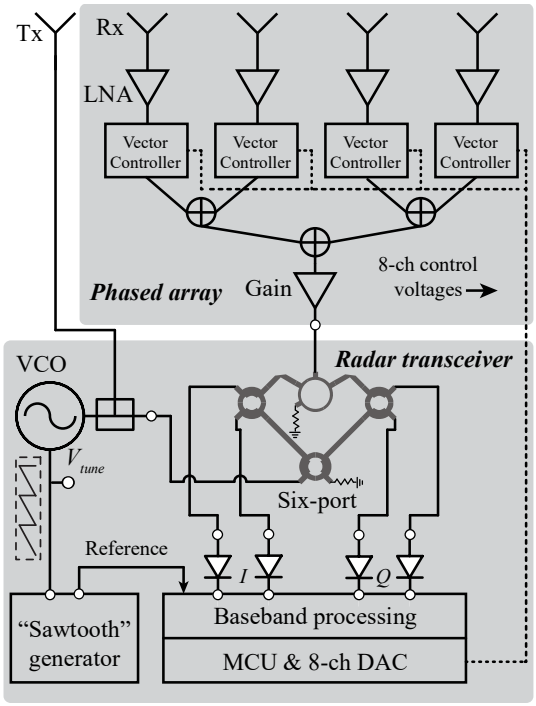

Fig. 1. Top-level block diagram of the proposed radar system with continuous beam steering phased array.

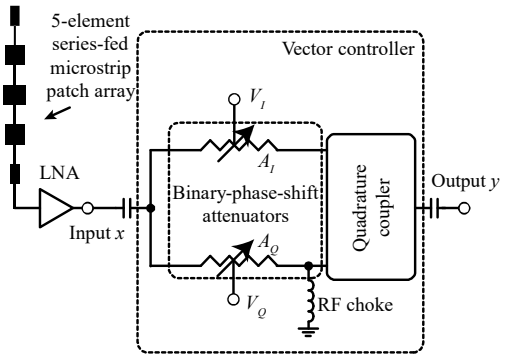

Fig. 2. One channel of the phased array.

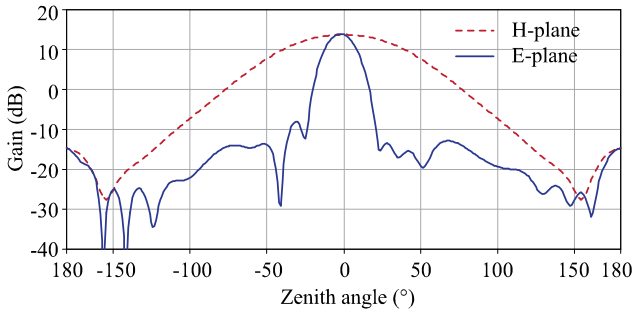

Fig. 3. H-plane and E-plane pattern of a 5-element series-fed microstrip patch array.

array, a six-port circuit and a baseband circuit. The phased array is a 4-element linear array. Each element is a series-fed microstrip patch array antenna. The beam of the phased array can be continuously steered with a range of ±30° on H-plane through an array of vector controllers. The vector controller is based on the concept of vector sum [17], [18] with binary-phase-shift attenuators. Each vector controller is capable to control the phase and the amplitude of the corresponding array element of the 4-element linear array. The beat signal of the FMCW radar is detected by the six-port circuit and then sampled by a soundcard of a laptop. The whole radar system is fabricated on printed circuit boards (PCB). The design principle of the array, the vector and the binary-phase-shift attenuator are illustrated. Characteristics of the binary-phase-shift and the vector controller are measured. In order to compensate the fabrication errors of the PCB and variation of components, a calibration method of the phased array is detailed. The radiation patterns of the phased array steered to different directions have been measured. Finally, an experiment of the whole radar system has been performed to reveal its capability in the applications of short-range localization.

The rest of the paper is organized as follows. Section II presents the design principles of the proposed radar system. In Section III, experiments were taken to demonstrate the calibration procedure of the phased array, and the patterns of the phased array steered to different angles have also been measured. Section IV describes an experiment, showing the capability of the proposed radar system for short-range localization. Finally, a conclusion is drawn in Section V.

II. Design Principles

This section presents the design principles of each part of the proposed radar system. Fig. 1 illustrates the top level block diagram of the proposed radar system. As shown in Fig. 1, in the transmitter channel, a "sawtooth" voltage sequence is generated by the "sawtooth" generator [27]. This "sawtooth" voltage sequence is used to control a free-running VCO to generate a frequency-modulated RF signal. Half of this signal is transmitted by a transmitter antenna and the other half is used as a local oscillator to drive the six-port circuit. Regarding the receiver channel, the phased array receives the signal reflected by targets, and then a six-port circuit is used to detect the beat signal. The beat signal is processed by a baseband circuit and sampled by the soundcard of a laptop. The phased array is a 4-element linear array. The beam of the phased array can be continuously steered on the H-plane through an array of vector controllers. The vector controllers are controlled by an 8-channel DAC, which is driven by a microcontroller (MCU).

Baseband signal processing has been reported in [27], in which a reference pulse sequence is used to align the phase of each beat signal and maintain the coherence of radar system.

A. Phased Array

Typically, in a transceiver system, a phased array can be used in the transmitter or in the receiver. For phased array designed in this paper, if it is used in the transmitter, the RF amplifiers used in the array should be able to handle relatively high power levels (above 0 dBm) in order to maintain enough transmit power. In this case, the linearity requirement for the RF amplifiers is difficult to be satisfied especially in K-band.

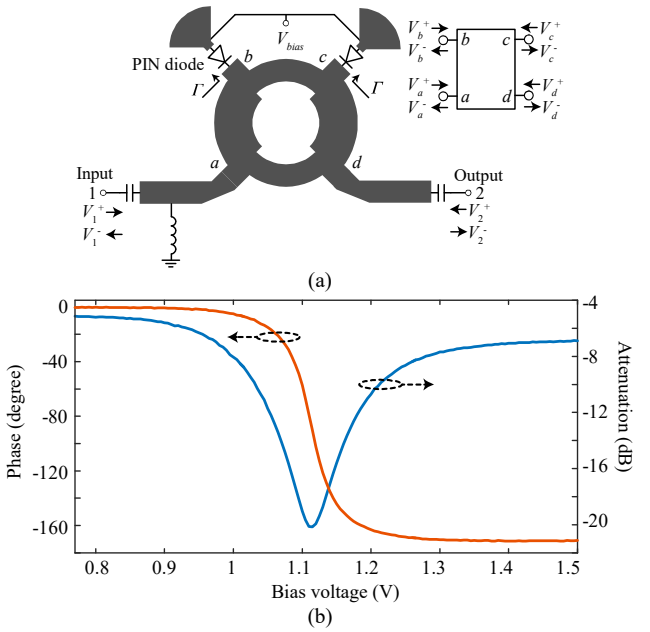

Fig. 4. (a) Schematic of the binary-phase-shift attenuator. (b) Measured amplitude and phase response to different bias voltages.

Therefore, this work has a single patch antenna on the transceiver side and a phased array on the receiver side.

The phased array in the proposed radar system is designed to be steerable on the H-plane and fixed on the E-plane on the receiver channel, and a single patch antenna is used as the transmitter antenna, which can simplify the structure of the RF frontend. The fundamental theory of the proposed phased array is based on the authors' previous work [29]. The proposed phased array in this radar system is a 4-element linear array. The distance between adjacent elements is $3\lambda/4$. Each array element is a 5-element series-fed microstrip patch array antenna. Fig. 2 demonstrates one channel of the proposed phased array, which has a 5-element series-fed microstrip patch array, a low noise amplifier (LNA) and a vector controller cascaded in sequence. The vector controller has a pair of binary-phase-shift attenuators, a power divider and a quadrature coupler.

1) Antenna

The 5-element series-fed microstrip patch array antenna is designed with a narrow beam width on the E-plane and a wide beam width on the H-plane. The layout of the antenna is shown in Fig. 2. Fig. 3 shows the simulated patterns of the H-plane and the E-plane. The gain of a single 5-element series-fed microstrip patch array is 13.9 dB. The beam width on the E-plane is 18.4°, and the beam width on the H-plane is 70.7°.

2) Binary-Phase-Shift Attenuator

The binary-phase-shift attenuator is the key component in the vector controller. The schematic of the binary-phase-shift attenuator is illustrated in Fig. 4(a). The attenuator is designed based on a quadrature coupler, which has two PIN diodes terminating ports *b* and *c*, respectively, with proper matching structures and bias circuits. Ports *a* and *d* are the input and output ports, respectively. The relation of the reflected voltage waves, incident voltage waves and the S-matrix of an ideal quadrature coupler can be written as:

$$\begin{bmatrix} V_a^- \\ V_b^- \\ V_c^- \\ V_d^- \end{bmatrix} = \begin{bmatrix} S_{aa} & S_{ab} & S_{ac} & S_{ad} \\ S_{ba} & S_{bb} & S_{bc} & S_{bd} \\ S_{ca} & S_{cb} & S_{cc} & S_{cd} \\ S_{da} & S_{db} & S_{dc} & S_{dd} \end{bmatrix} \begin{bmatrix} V_a^+ \\ V_b^+ \\ V_c^+ \\ V_d^+ \end{bmatrix} \quad (1)$$

where $S_{ab} = S_{ba} = S_{cd} = S_{dc} = -j/\sqrt{2}$, $S_{ac} = S_{ca} = S_{bd} = S_{db} = -1/\sqrt{2}$, and $S_{aa} = S_{bb} = S_{cc} = S_{dd} = S_{ad} = S_{da} = S_{cd} = S_{dc} = 0$ for an ideal quadrature coupler. V^- is the reflected voltage wave at each port, and V^+ is the incident voltage wave of the corresponding port. Based on the connection shown in Fig. 4(a), the reflection coefficient of an ideal PIN diode is $\Gamma = V_b^+/V_b^- = V_c^+/V_c^-$.

The S-matrix of the binary-phase-shift attenuator can be expressed as:

$$\begin{bmatrix} V_1^- \\ V_2^- \end{bmatrix} = \begin{bmatrix} V_a^- \\ V_d^- \end{bmatrix} = \begin{bmatrix} S_{11} & S_{12} \\ S_{21} & S_{22} \end{bmatrix} \begin{bmatrix} V_a^+ \\ V_d^+ \end{bmatrix} = \boldsymbol{S_{atten}} \begin{bmatrix} V_1^+ \\ V_2^+ \end{bmatrix} \quad (2)$$

where $\boldsymbol{S_{atten}}$ is the S-matrix of the attenuator. Combining (1) and (2), the S-parameter of the attenuator can be derived as:

$$S_{11} = S_{22} = \frac{V_1^-}{V_1^+} = \frac{-jV_b^+ - V_c^+}{\sqrt{2}V_1^+} \quad (3)$$

$$S_{21} = S_{12} = \frac{V_2^-}{V_1^+} = \frac{\Gamma(-V_b^+ - jV_c^+)}{jV_b^+ - V_c^+} = j\Gamma \quad (4)$$

For an ideal quadrature coupler, $V_c^+ = -jV_b^+$, thus, S_{11}=S_{22}=0, i.e., the input and output of the attenuator are matched. The attenuation and phase shift of the attenuator are:

$$|S_{21}| = |\Gamma| \quad (5)$$

$$\angle S_{21} = \pi/2 + \pi\text{sign}(\Gamma)/2. \quad (6)$$

It is known that the resistance of an ideal PIN diode varies according to its forward bias current and can range from 0 Ω to hundreds of Ω. Thus the reflection coefficient Γ of an ideal PIN diode, without considering parasitics, varies approximately from -1 to 1. According to (5), When the resistance is 50 Ω, Γ =0 for a 50 Ω system, which results in the maximum attenuation from port 1 to port 4 for the circuit in Fig. 4(a).

From (6), there are two phase states for this attenuator, i.e., 0° and 180°, achieving binary phase shift required for the proposed vector controller. However, parasitics and PCB fabrication errors introduce an error between the binary phase states. For example, Fig. 4(b) is the measured results of a prototype binary-phase-shift attenuator at 24.5 GHz with bias voltage increasing from 770 mV to 1500 mV. A phase difference of 170° is achieved for the binary phase states, and the attenuation ranges from -6.5 dB to -20 dB.

3) Vector Controller

The block diagram of the vector controller is shown in Fig. 2. The input RF signal is divided into two channels, and each channel has a binary-phase-shift attenuator, which has two phase states, i.e., 0° and 180°. After the attenuators, these two channels are combined with a quadrature coupler. DC block

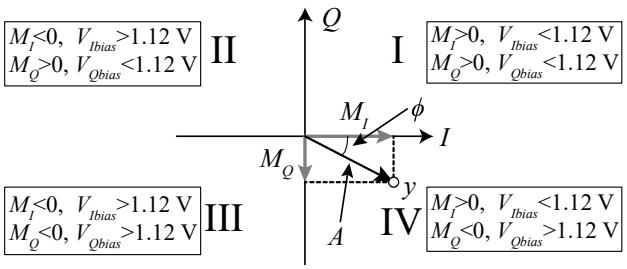

Fig. 5. Distribution of the output signal on a constellation disgram.

capacitors and bias circuits are added to control the bias currents of the PIN diodes.

For an input signal $x = \sin(2\pi f_c t)$ passing through the vector controller, the output y can be written as:

$$y = M_I \sin(2\pi f_c t) + M_Q \cos(2\pi f_c t) = \mathrm{Re}\{Ae^{j\phi} e^{-j2\pi f_c t}\} \quad (7)$$

where f_c is the carrier frequency, $M_I = \pm A_I/2$ and $M_Q = \pm A_Q/2$, and A_I, A_Q are the attenuations of the two attenuators. The signs of M_I and M_Q are determined by the phase states of the two attenuators, i.e., M_I and M_Q are positive when phase state is 0° and negative when phase state is 180°. As shown in Fig. 5, the output y can be mapped to the constellation diagram. The radius A between point y and the origin in Fig. 5 is the output amplitude, and the angle ϕ is the output phase shift:

$$A = \sqrt{M_I^2 + M_Q^2} \quad (8)$$

$$\phi = \arctan\frac{M_Q}{M_I} \quad (9)$$

Based on the characteristic of the binary-phase-shift attenuator, output distribution of the vector controller related to the bias voltages can be marked in Fig. 5. The output signal y is distributed in all the four quadrants, which means it is possible to adjust the phase and amplitude simultaneously by changing the bias voltages of the attenuators, and the phase shift range is 360°.

A prototype of the vector controller has been designed and fabricated, as shown in Fig. 6. The substrate of the PCB board is Rogers RT/duroid 5880 with a thickness of 0.254 mm. The flip-chip PIN diode used in the prototype is MACOM MADP-000907-14020, whose parasitic capacitance is smaller than 0.03 pF. The board is 23 mm × 36 mm.

Measured results of the prototype at 24.5 GHz are shown in Fig. 7. Each point in the constellation diagram represents a S_{21} result at certain control voltages V_I and V_Q. The voltage sweep range for both attenuators is between 700 mV and 1500 mV with a 10-mV step size. For every single point in the constellation diagram, the radius A corresponds to the attenuation of the vector controller in linear scale, and the angle ϕ represents the phase shift of the vector controller. Since the points are distributed in all the four quadrants, the phase shift range of the proposed vector controller can reach to 360°. The measured results match with the analysis.

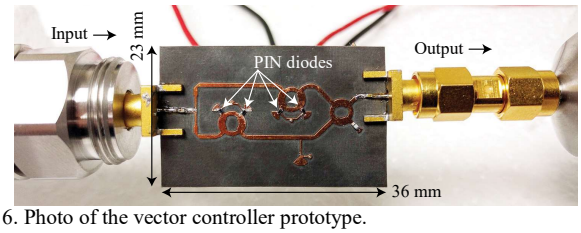

Fig. 6. Photo of the vector controller prototype.

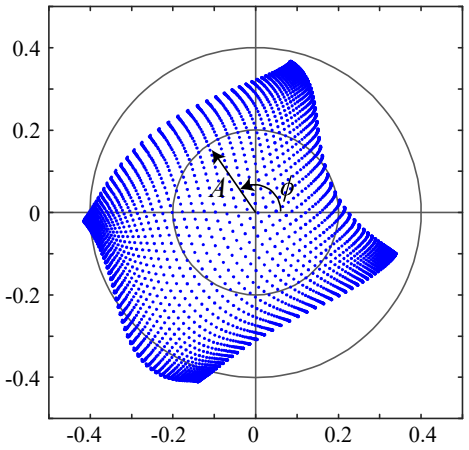

Fig. 7. Measured constellation diagram of the vector controller at 24 GHz (voltage swept between 770 mV and 1500 mV with a 10-mV step for both attenuators).

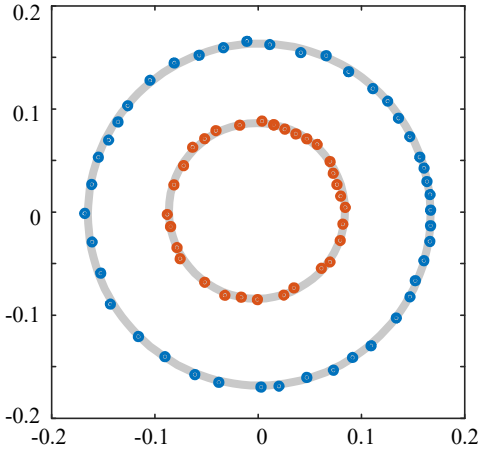

Fig. 8. Two concentric circles extracted from Fig. 7.

Fig. 8 shows two extracted circles from Fig. 7. Each circle has a different constant attenuation. The function of the vector controller in each circle is identical to a simple phase shifter, which has a phase shift range of 360°. By simply modifying the bias voltages, more concentric circles can be extracted from Fig. 7, which means 0° to 360° phase shifts with different attenuations can be obtained.

B. FMCW radar

As shown in Fig. 1, a free running VCO controlled by V_{tune} generates a K-band frequency modulated RF signal [27], which is transmitted by a single patch antenna. The K-band frequency modulated RF signal also drives a six-port circuit to down-convert the received signal and obtain the differential quadrature baseband signal. Design considerations of six-port parameters can be found in the literatures [30], [31]. The VCO

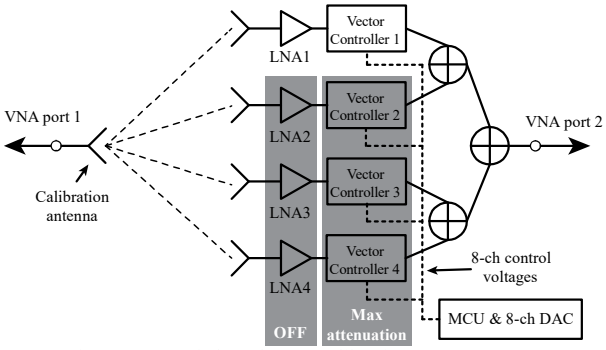

Fig. 9. Experiment setup of phased array calibration.

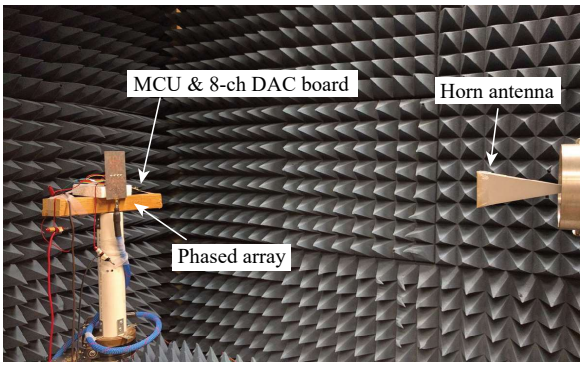

Fig. 10. Experiment environment of the pattern measurement for the phased array.

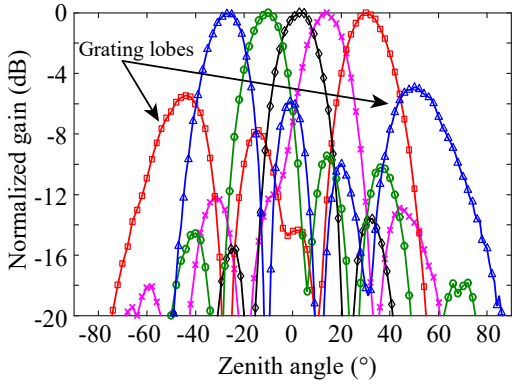

Fig. 11. Measured patterns of the phased array steered to different angles at 24.5 GHz.

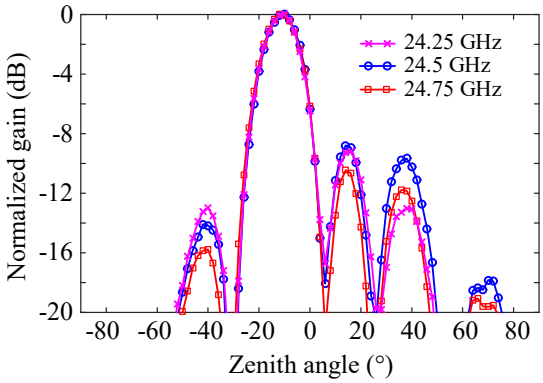

Fig. 12. Measured patterns when the phased array is steered to -15° at different frequencies.

TABLE I
CONTROL VOLTAGES TO OBTAIN THE PATTERNS IN FIG. 11.

Angle	Channel 1		Channel 2		Channel 3		Channel 4	
	V_I (mV)	V_Q (mV)	V_I (mV)	V_Q (mV)	V_I (mV)	V_Q (mV)	V_I (mV)	V_Q (mV)
-30°	1066	1040	1163	1220	1310	1060	970	1110
-15°	1066	1040	1080	1160	1144	1240	1500	1170
0°	1066	1040	1064	1030	1058	1042	1064	1044
15°	1053	1024	1150	1030	1380	1095	1166	1178
30°	1053	1024	1280	1103	1084	1132	1107	950

control voltage V_{tune} is generated by a pair of operational amplifiers. A reference signal generated at the same time with the V_{tune} voltage is used to align the phase of each beat signal detected by the FMCW radar, and thus keeping the radar system coherent. To simplify the system, a soundcard from a laptop is used to acquire the baseband beat signal as well as the reference signal. The line-in mode of the soundcard is used, so that the soundcard can acquire two channels at the same time. One channel of the soundcard is the reference signal and the other channel can be either I channel or Q channel baseband output from the down-converter. As FMCW radars do not require quadrature demodulation, one channel of I/Q baseband output is sufficient to obtain the target range information. All the signal processing procedures, including aligning the phase of each beat signal, are accomplished in the laptop.

III. ARRAY CALIBRATION AND PATTERN MEASUREMENT

In order to control the phase of each array element, typically, there are two methods to obtain the relations among the phase shift ϕ, the attenuation A, and the control voltages, i.e., V_I and V_Q. The first method is using a polynomial to fit the curves in Fig. 4(b), which seems to be easy to execute but is not reliable due to fabrication errors, component variations and soldering variations for a PCB level implementation at 24 GHz. The other method relies on a calibration procedure to establish a look-up table, which can minimize the errors caused by fabrications, component variations and soldering variations.

A. Array Calibration

Array calibration requires a vector network analyzer (VNA) and a calibration antenna, denoted as "probe antenna" henceforth. In the setup, the calibration antenna and the phased array are placed face-to-face. The calibration procedure is described as follows:

1) Turn on all the 4 LNAs and tune the eight control voltages to get the minimum magnitude of S_{21}, which means each vector controller is in the "maximum attenuation" state. Record the value of each control voltage.
2) Assuming the signal phase delay from the receiver antennas to VNA port 2 is the same for each channel in the initial state (with LNAs turned on and V_I=V_Q=0), which is guaranteed during the design of the phased array by making sure the length of microstrip lines of different channels are the same, record the phase of each channel in the initial state.
3) Obtain the relative phase shift as a function of control

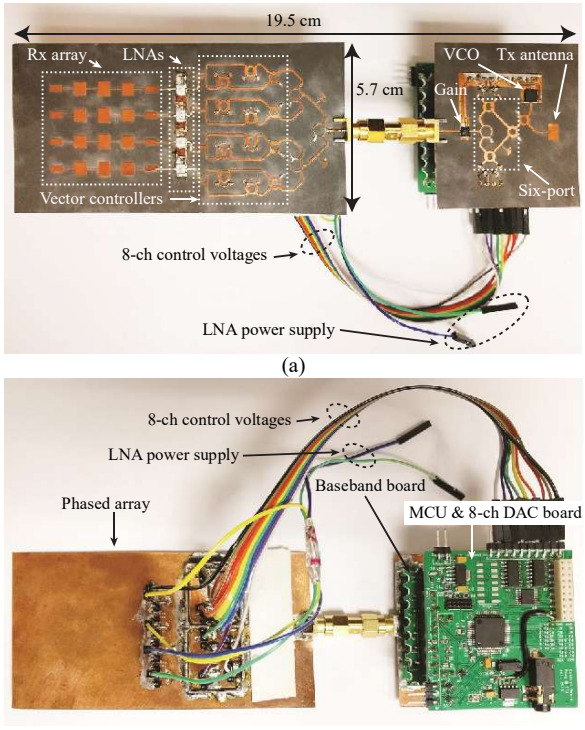

Fig. 13. Photos of the proposed radar prototype. (a) Top view. (b) Bottom view.

TABLE II
LIST OF COMPONENTS OF THE PROPOSED RADAR SYSTEM

Radar Part	Device	Manufacturer	Function
Phased array	HMC341LC3B	Analog Devices	LNA
	MADP-000907-14020	MACOM	PIN diode
FMCW transceiver	HMC739LP4	Analog Devices	VCO
	MAAL-011111	MACOM	Gain
	SMS7621-040LF	Skyworks	Schottky diode
Baseband	ADA4851	Analog Devices	OpAmp
	AD5668	Analog Devices	DAC
	MSP430	TI	MCU

voltages for each individual channel. The relative phase shift is obtained by comparing the instant phase shift with that measured in the initial state. In this step, the LNAs of other channels are turned off and the vector controllers of the other channels are in the maximum attenuation state. Fig. 9 shows the configuration when calibrating channel 1.

In this radar system, the beam steering step is set to 2.5° with maximum steering angle of ±30°. Though the vector controllers have the ability to simultaneously control the phase and amplitude, in this work, only the phase control function is used. After calibration, a look-up table with 25 × 8 control voltages is created.

It should be noted that this calibration method minimizes errors introduced by fabrications, component variations and soldering variations. However, there is still residual errors, such as that due to the assumption of equal phase delays in the initial state. Coupling between adjacent antennas will also introduce phase shift. Despite these errors, the proposed calibration method minimizes the major uncertainty in controlling the phased array.

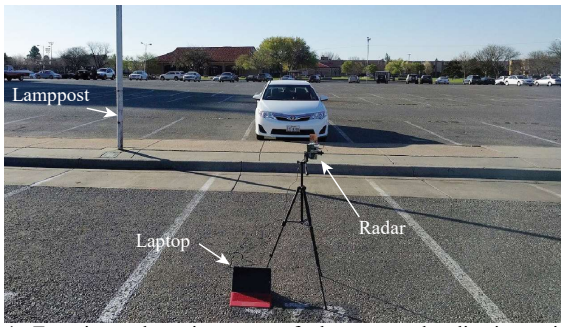

Fig. 14. Experimental environment of short-range localization using the proposed radar prototype.

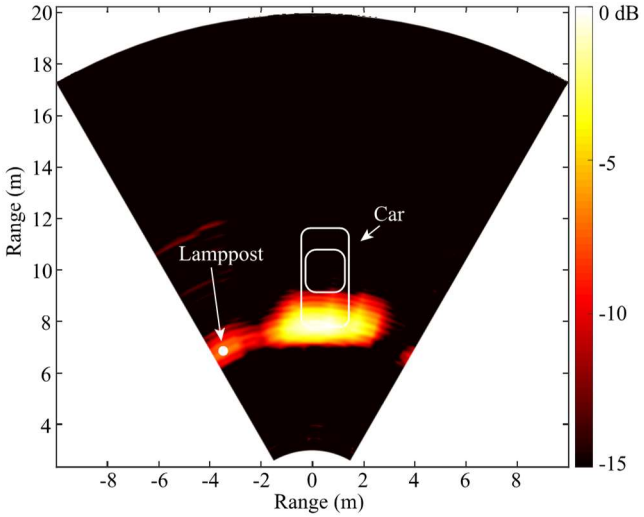

Fig. 15. Measured result of the short-range localization experiment using the proposed radar prototype.

B. Pattern Measurement

In order to verify the performance and steering capability of the phased array, experiments have been taken to measure the far-field patterns of the phased array with different steering angles. Fig. 10 shows the measurement environment in a microwave anechoic chamber. The distance between the phased array and the standard horn antenna is about 1 m. During the experiment, the phased array was turned from -90° to 90° with a 2° step on a turntable.

Measured patterns of the phased array steered to different angles are illustrated in Fig. 11. Patterns with 5 different angles, i.e., -30°, -15°, 0°, 15° and 30°, were plotted at the frequency of 24.5 GHz. The corresponding control voltages to obtain the 5 patterns are listed in Table I.

In this design, the steering range is limited to ±30°, which can be observed in Fig. 10. The main limitation of the steering range is due to the distance between adjacent array elements, which is $3\lambda/4$. When the beam is tuned to 30° or -30°, a major grating lobe appears, as shown in Fig. 11. In order to further increase the steering range of the array, the distance between adjacent array element should be reduced, which can be achieved using substrate materials with higher dielectric

constant or patch miniaturization techniques [32].

Regarding the bandwidth of the phased array, the measured patterns of the array steered to -15° at different frequencies is illustrated in Fig. 12. The patterns of the phased array at the frequencies of 24.25 GHz, 24.5 GHz and 24.75 GHz are consistent, which means the proposed phased array has a bandwidth from 24.25 GHz to 24.75 GHz.

IV. Radar System Experiment

Experiment with the proposed radar system has been performed in a short-range localization demonstration. Fig. 13 is the photo of the proposed radar system. The entire radar prototype has a size of 19.5 cm × 5.7 cm and weighs 69 grams. The substrate material used for the RF board is Rogers RT/duroid 5880 and the substrate material for the baseband board is FR4. Table II lists the main components used in the radar prototype. In the phased array, the LNAs are Analog Devices HMC341LC3B, and the PIN diodes are MACOM MADP-000907-14020. In the FMCW radar transceiver part, the VCO is Analog Devices HMC739LP4, the gain block is MACOM MAAL-011111 and the Schottky diodes are Skyworks SMS7621-040LF. The main components in the baseband are the operational amplifiers (Analog Devices ADA4851), the DAC (Analog Devices AD5668) and the MCU (TI MSP430).

The short-range localization experimental setup is shown in Fig. 14. In the radar's field of view, a car was located in front and a lamppost was located beside the car. The scanning angle step was 2.5°. The radar system was powered by a single 9-V battery. The period of the "sawtooth" sequence is 2.3 ms, i.e., the chirp repetition period is 2.3 ms. The transmitted signal has a bandwidth of 500 MHz from 24.25 GHz to 24.75 GHz with an average power of 8 dBm. The voltage gain of the receiver chain is 56 dB. The soundcard of a laptop was used to sample the baseband signal with a sampling rate of 192 ksps. All the data was processed in the laptop. The measured result of the short-range localization experiment is illustrated in Fig. 15. The locations of the car and the lamppost were detected.

V. Conclusions

A 24-GHz portable FMCW radar with continuous beam steering phased array is proposed in this paper. The proposed radar system is designed and fabricated on PCB using off-the-shelf components. The radar system includes both the transmitter and receiver channels operating at the frequency from 24.35 GHz to 24.75 GHz. The transmitter channel consists of a VCO and a single patch antenna. The VCO is controlled by a "sawtooth" voltage to generate frequency-modulated RF signal. In the receiver channel, a novel phased array using vector controllers that eliminate the requirement on RF phase shifters is designed, fabricated and measured. The design principles of the phased array based on vector controllers has been presented. In addition, a calibration procedure for the phased array is introduced to minimize the errors caused by fabrication and components variation. The beam of the phased array can be continuously steered within a range of ±30° on the H-plane. A six-port circuit is used in the receiver channel to detect the beat signal of the FMCW radar, which is then sampled by the soundcard of a laptop. The radiation patterns of the phased array steered to different directions have been measured. Experiments of the whole radar system have been performed to reveal its capability in short-range localization.

Acknowledgement

Z. Peng and C. Li would like to acknowledge Dr. M. Saed and Mr. A. Alajmi for their help in measuring the radiation pattern of the phased array.

References

[1] D. M. Grimes and T. O. Jones, "Automotive radar: A brief review," *Proc. IEEE*, vol. 62, no. 6, pp. 804-822, Jun. 1974.

[2] J. Hasch, E. Topak, R. Schnabel, T. Zwick, R. Weigel, and C. Waldschmidt, "Millimeter-wave technology for automotive radar sensors in the 77 GHz frequency band," *IEEE Trans. Microw. Theory Techn.*, vol. 60, no. 3, pp. 845-860, Mar. 2012.

[3] M. Vossiek, L. Wiebking, P. Gulden, J. Wieghardt, C. Hoffmann, and P. Heide, "Wireless local positioning," *IEEE Microw. Mag.*, vol. 4, no. 4, pp. 77-86, Dec. 2003.

[4] F. Ahmad and M. G. Amin, "Noncoherent approach to through-the-wall radar localization," *IEEE Trans. Aerosp. Electron. Syst.*, vol. 42, no. 4, pp. 1405-1419, Oct. 2006.

[5] D. Sto, "Through wall imaging: Historical perspecitve and future directions," in *IEEE Int. Conf. on Acoust., Speech and Signal Process.*, Las Vegas, NV, Mar. 2008, pp. 5173-5176.

[6] C. Li, V. M. Lubecke, O. Boric-Lubecke, and J. Lin, "A Review on Recent Advances in Doppler Radar Sensors for Noncontact Healthcare Monitoring," *IEEE Trans. Microw. Theory Techn.*, vol. 61, no. 5, pp. 2046-2060, May 2013.

[7] R. Rotman, "Recent advances using microwaves for imaging, hyperthermia and interstitial ablation of breast cancer tumors," in *IEEE Int. Conf. on Microwaves, Commun., Antennas and Electron. Syst. (COMCAS)*, Tel Aviv, Nov. 2011, pp. 1-4.

[8] T. Elmissaoui, N. Soudani, and R. Bouallegue, "UWB radar for medical applications," in *12th Int. Radar Symp. (IRS),* Leipzig, Sep. 2011, pp 526-531.

[9] H. J. Visser, *Array and Phased Array Antenna Basics*, 2006. Wiley

[10] M. S. Lee and Y. H. Kim, "Design and performance of a 24-GHz switch-antenna array FMCW radar system for automotive applications," *IEEE Trans. Veh. Technol.*, vol. 59, no. 5, pp. 2290-2297, Jun. 2010.

[11] W. Lee, J. Kim, and Y. J. Yoon, "Compact two-layer rotman lens-fed microstrip antenna array at 24 GHz," *IEEE Trans. Antennas Propag.*, vol. 59, no. 2, pp. 460-466, Feb. 2011

[12] M. Morinaga, T. Nagasaku, H. Shinoda, and H. Kondoh, "24GHz intruder detection radar with beam-switched area coverage," in *IEEE MTT-S Int. Microwave Symp. Dig.*, Honolulu, HI, Jun. 2007, pp. 389-392.

[13] H. Hashemi, X. Guan, A. Komijani, and A. Hajimiri, "A 24-GHz SiGe phased-array receiver - LO phase-shifting approach," *IEEE Trans. Microw. Theory Techn.*, vol. 53, no. 2, pp. 614-625, 2005.

[14] X. Guan, H. Hashemi, and A. Hajimiri, "A fully integratted 24-GHz eight-element phased-array receiver in silicon," *IEEE J. Solid-State Circuits*, vol. 39, no. 12, pp. 2311-2320, 2004.

[15] T. Yu and G. M. Rebeiz, "A 22-24 GHz 4-element CMOS phased array with on-chip coupling characterization," *IEEE J. Solid-State Circuits*, vol. 43, no. 9, pp. 2134-2143, Sep. 2008.

[16] C.-W. Wang, H.-S. Wu, and C.-K. C. Tzuang, "CMOS Passive Phase Shifter With Group-Delay Deviation of 6.3 ps at K-Band," *IEEE Trans. Microw. Theory Techn.*, vol. 59, no. 7, pp. 1778-1786, Jul. 2011.

[17] P.-Y. Chen, T.-W. Huang, H. Wang, Y.-C. Wang, C.-H. Chen, and P.-C. Chao, "K-Band HBT and HEMT Monolithic Active Phase Shifters Using Vector Sum Method," *IEEE Trans. Microw. Theory Techn.*, vol. 52, no. 5, pp. 1414-1424, May 2004.

[18] P. S. Wu, H. Y. Chang, M. Da Tsai, T. W. Huang, and H. Wang, "New miniature 15-20-GHz continuous-phase/amplitude control MMICs using 0.18-μm CMOS technology," *IEEE Trans. Microw. Theory Techn.*, vol. 54, no. 1, pp. 10-18, Jan. 2006.

[19] Z. Peng, J. Chen, Y. Dong, B. Zhang, D. Ye, J. Huangfu, Y. Sun, C. Li, L. Ran, "Radio Frequency Beamforming Based on a Complex Domain Frontend," *IEEE Trans. Microw. Theory Techn*, vol. 64, no. 1, pp. 289-298, Jan. 2016.
[20] T. Mitomo, N. Ono, H. Hoshino, Y. Yoshihara, O. Watanabe, and I. Seto, "A 77 GHz 90 nm CMOS transceiver for FMCW radar applications," *IEEE J. Solid-State Circuits*, vol. 45, no. 4, pp. 928-937, Apr. 2010.
[21] S. Scheiblhofer, S. Schuster, and A. Stelzer, "High-speed FMCW radar frequency synthesizer with DDS based linearization," *IEEE Microw. Compon. Lett.*, vol. 17, no. 5, pp. 397-399, May 2007.
[22] N. Pohl, T. Jaeschke, and K. Aufinger, "An ultra-wideband 80 GHz FMCW radar system using a SiGe bipolar transceiver chip stabilized by a fractional-N PLL synthesizer," *IEEE Trans. Microw. Theory Techn.*, vol. 60, no. 3, pp. 757-765, Mar. 2012.
[23] T. Musch, "A high precision 24-GHz FMCW radar based on a fractional-N ramp-PLL," *IEEE Trans. Instrum. Meas.*, vol. 52, no. 2, pp. 324-327, Apr. 2003.
[24] S. O. Tatu and K. Wu, "Six-port technology and applications," in *11th Int. Conf. on Telecommun. in Modern Satellite, Cable and Broadcasting Services (TELSIKS)*, Nis, Oct. 2013, vol. 01, pp. 239-248.
[25] G. Vinci, S. Lindner, F. Barbon, S. Mann, M. Hofmann, A. Duda, R. Weigel, and A. Koelpin, "Six-port radar sensor for remote respiration rate and heartbeat vital-sign monitoring," *IEEE Trans. Microw. Theory Techn.*, vol. 61, no. 5, pp. 2093-2100, May 2013.
[26] G. Vinci, S. Lindner, F. Barbon, M. Hofmann, G. Fischer, D. Kissinger, and A. Koelpin, "24 GHz six-port medical radar for contactless respiration detection and heartbeat monitoring," in *Proc. of the 9th European Radar Conf. (EuRAD)*, Amsterdam, Oct. 2012, pp. 75-78.
[27] Z. Peng and C. Li, "A portable 24-GHz FMCW radar based on six-port for short-range human tracking," in *IEEE MTT-S 2015 Int. Microwave Workshop Series on RF and Wireless Technologies for Biomedical and Healthcare Applications (IMWS-BIO),* Taipei, Sep. 2015, pp. 81-82.
[28] H. Zhang, L. Li, and K. Wu, "Software-defined six-port radar technique for precision range measurements," *IEEE Sensors J.*, vol. 8, no. 10, pp. 1745-1751, Oct. 2008.
[29] Z. Peng, L. Lixin Ran, and C. Li, "A 24-GHz low-cost continuous beam steering phased array for indoor smart radar," in *2015 IEEE 58th Int. Midwest Symp. on Circuits and Systems (MWSCAS)*, Fort Collins, CO, Aug. 2015, pp. 1-4.
[30] S. Linz, G. Vinci, S. Lindner, S. Mann, F. Lurz, F. Barbon, R. Weigel, and A. Koelpin, "I/Q imbalance compensation for Six-port interferometers in radar applications," in *European Microwave Week 2014: Connecting the Future (EuMC),* Rome, Oct. 2014, pp. 746-749.
[31] A. Stelzer, C. G. Diskus, and R. Weigel, "Accuracy considerations and FMCW operation of a six-port device," in *Asia-Pacific Microwave Conf. (APMC)*, Taipei, Dec. 2001, vol. 2, pp. 407-410.
[32] K. L. Wong, *Compact and Broadband Microstrip Antennas*. New York, NY, USA: Wiley, 2002, pp. 1-2-22-39.

Zhengyu Peng (S'15) received the B.S. degree in Electrical Engineering from Zhejiang University, Hangzhou, China, in 2011, and the M.Sc. degree in Electrical Engineering from Zhejiang University, Hangzhou, China, in 2014.

He is currently working towards the Ph.D. degree in Electrical Engineering in Texas Tech University (TTU), Lubbock, TX, USA. His research interests include antennas, microwave circuits, and biomedical applications of microwave/RF circuits and systems.

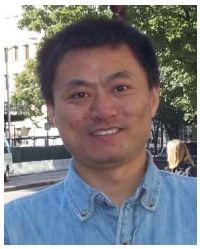

Lixin Ran received his BS, MS and PhD degrees from Zhejiang University, in 1991, 1994 and 1997, respectively. He became an assistant professor in 1997, an associate professor in 1999 and a full professor in 2004, all with the Department of Information and Electronics Engineering, Zhejiang University. He is the Director of the Laboratory of Applied Research on Electromagnetics (ARE).

In 2005, 2009 and 2012, he visited Massachusetts Institute of Technology as a visiting scientist. He is the co-author of over 120 research papers published in peer-reviewed journals, and the inventor of over 30 licensed patents. His research interests include new concept antennas, radio-aware sensing and imaging, radio frequency, microwave and terahertz systems and artificial active media.

Changzhi Li (S'06-M'09-SM'13) received the B.S. degree in Electrical Engineering from Zhejiang University, China, in 2004, and the Ph.D. degree in Electrical Engineering from the University of Florida, Gainesville, FL, in 2009.

In the summers of 2007-2009, he was with Alereon inc. Austin, TX, USA, and Coherent Logix inc. Austin, TX, USA, where he was involved with ultra-wideband (UWB) transceivers and software-defined radio. He joined Texas Tech University as an Assistant Professor in 2009, and became an Associate Professor in 2014. His research interests include biomedical applications of microwave/RF, wireless sensor, and analog circuits.

Dr. Li is an associate editor for the *IEEE Transactions on Circuits and Systems I*. He served as an associate editor for the *IEEE Transactions on Circuits and Systems II* in 2014 and 2015. He served as the TPC co-chair for the *IEEE Wireless and Microwave Technology Conference (WAMICON)* in 2012 and 2013. He received the ASEE Frederick Emmons Terman Award in 2014, the IEEE-HKN Outstanding Young Professional Award in 2014, the NSF Faculty Early CAREER Award in 2013, and the IEEE MTT-S Graduate Fellowship Award in 2008. He received a few best paper awards as author/advisor in IEEE-sponsored conferences.